

From Isodesmic to Highly Cooperative: Reverting Supramolecular Polymerization Mechanism in Water by Fine Monomer Design.

Received 00th January 20xx,
Accepted 00th January 20xx

Nicolas M. Casellas,^a Sílvia Pujals,^d Davide Bochicchio,^e Giovanni M. Pavan,^e Tomás Torres,^{*,a,b,c}
Lorenzo Albertazzi^{*,d} and Miguel García-Iglesias^{*,a,b}

DOI: 10.1039/x0xx00000x

www.rsc.org/

Two structurally-similar discotic molecules able to self-assemble in water forming supramolecular fibers are reported. While both self-assembled polymers are indistinguishable from a morphological point-of-view, a dramatic change in their polymerization mechanism is observed (i.e., one self-assemble via an isodesmic mechanism while the other shows one of the highest cooperativities values).

The rational design of building blocks able to self-assemble into stable but still dynamic ordered structures in water is of utmost importance towards the use of supramolecular materials for many applications, in particular in the biomedical field.¹ To this goal, different molecular interactions have to be mastered, such as solvophobic effects, π - π stacking, and hydrogen bonding. For supramolecular polymers, it has been observed that little changes in the molecular structure lead to unpredicted changes in the structural and dynamic behavior of the aggregates.² For this reason the rational design of supramolecular 1-dimensional aggregates in water is still extremely challenging and a better understanding of the interactions driving self-assembly is crucial.³ Two main mechanisms of supramolecular polymerization are known: isodesmic and cooperative.⁴ The determinants of such process are several including dipole interactions,⁵ molecular order⁶ and a combination of several interactions⁷. Typically, a highly cooperative polymerization mechanism is desired, leading to longer and more monodisperse assemblies.^{7a} However,

although numerous supramolecular polymers have been reported,³ there are only few examples where mechanistic studies have been carried out in water,⁸ and consequently, the rational bases of the polymerization mechanism are still elusive. Herein we show the synthesis and self-assembly of two different C_3 -symmetric benzotrithiophene (BTT)⁹ units, into one-dimensional aggregates in water. The detailed experimental and computational study we present unveiled unexpected aspects of the polymerization process allowing for a rational understanding of the structure-mechanism relations. Figures 1a,f show the structure of the monomers **BTT-F** and **BTT-5F**, designed and synthesized for the generation of water-soluble supramolecular polymers (see ESI for synthetic procedure and characterization). The structure comprises an aromatic C_3 -symmetric BTT core providing robustness and rigidity to the columnar aggregates due to the combination of hydrophobic forces and π - π interactions. The aminoacids, L-phenylalanine (**BTT-F**) or pentafluoro-L-phenylalanine (**BTT-5F**), were attached to the core, providing directional hydrogen-bonding and non-directional hydrophobic interactions. Finally, in order to impart water solubility, octaethylene glycol side-chains were introduced next to the amino acid units in both compounds. Therefore, the two structures are endowed with the same geometry, core and PEG layer and differ only in the hydrophobicity of the amino acid, being **BTT-5F** more hydrophobic (see Fig. S1). A close inspection of **BTT-F** and **BTT-5F** aggregates by TEM negative staining confirms the formation of fibrillar assemblies in water. Images revealed the presence of structurally similar fibers with a diameter of 5 nm and few hundreds nm to μ m long. (see Figures 1b,g and S2). Moreover they show similar size as confirmed by DLS (see Fig. S3). Additionally, the two assemblies show nearly identical spectroscopical features in UV-VIS, fluorescence and CD measurements.

Both **BTT-F** and **BTT-5F** show a BTT core absorption band less intense and blue-shifted with respect to the absorption maximum observed in THF solutions, indicating the presence of stacking (e.g., between BTT cores, PHE amino acids, or both) in water¹⁰ (see Figures 1c,h).

^a Department of Organic Chemistry, Universidad Autónoma de Madrid (UAM), Calle Francisco Tomás y Valiente, 7, 28049 Madrid, ES. E-mail: tomas.torres@uam.es, miguel.iglesias@uam.es.

^b IMDEA Nanociencia, c/ Faraday 9, Cantoblanco, 28049, ES.

^c Institute for Advanced Research in Chemical Sciences (IAdChem), UAM, 28049 Madrid, ES.

^d Nanoscopy for Nanomedicine group, Institute for Bioengineering of Catalonia (IBEC), The Barcelona Institute of Science and Technology (BIST), Carrer Baldri Reixac 15-21, 08024 Barcelona, ES. E-mail: albertazzi@ibecbarcelona.eu

^e Department of Innovative Technologies, University of Applied Sciences and Arts of Southern Switzerland, Galleria 2, Via Cantonale 2c, CH-6928 Manno, CH. E-mail: giovanni.pavan@supsi.ch

Electronic Supplementary Information (ESI) available: [details of any supplementary information available should be included here]. See DOI: 10.1039/x0xx00000x

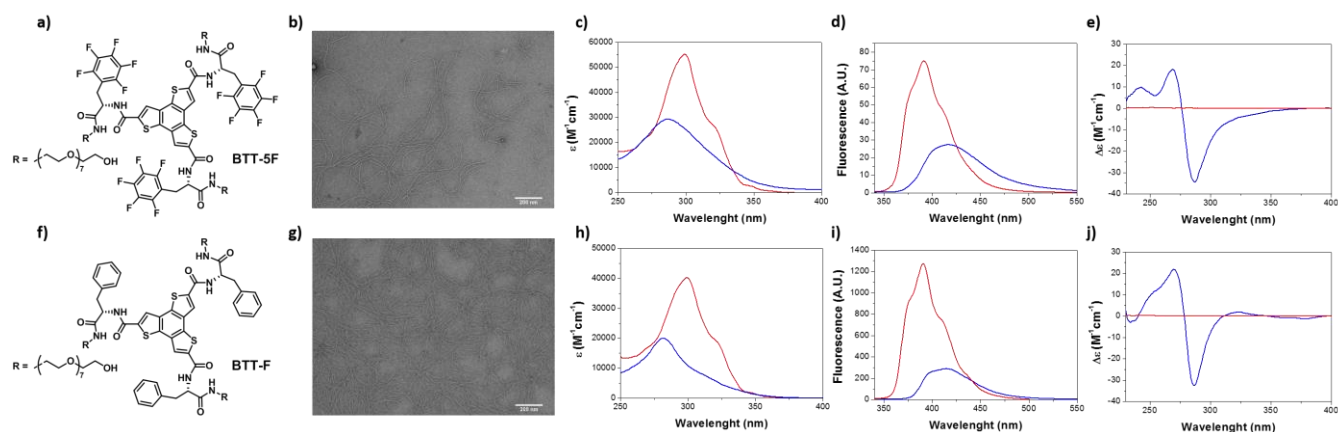


Fig. 1. Chemical structure of **BTT-5F** (a) and **BTT-F** (f). TEM images of **BTT-5F** (b) and **BTT-F** (g) one-dimensional fibers in water ($c = 4 \times 10^{-5}$ M). UV-vis absorption spectra, emission spectra ($\lambda_{\text{ex}} = 287$ nm), and CD spectra of **BTT-5F** (c, d, e) and **BTT-F** (h, i, j) in water (blue) and in THF (red) ($c = 4 \times 10^{-5}$ M) at room temperature.

Similar indications are provided by fluorescence spectroscopy, showing a bathochromic-shifted emission in water with respect to the THF solution. The lower emission intensity, together with the larger Stoke's shift shown in water (with respect to the molecularly dissolved state in THF) are clearly pointing to the formation of H- aggregates in both cases¹⁰ (see Figures 1d and i). **BTT-F** and **BTT-5F** self-assembly was also investigated by CD spectroscopy. While solutions of both compounds in THF remained CD silent, indicating lack of aggregation, solutions in water presented a similarly shaped bi-signed Cotton effect in their CD spectra (see Figures 1e and j). Summarizing, the two compounds assemble into 1-dimensional objects with indistinguishable mesoscopic and nanoscopic features.

In order to study the polymerization mechanism, temperature

dependent experiments in water were carried out from 283 to 353 K, monitoring changes to the UV, fluorescence and CD spectra as well as at the aggregate size by DLS. The lower critical solution temperature (LCST) of octaethyleneglycol side chains was observed above 355 K, representing the upper limit for temperature-dependent measurements. As shown in Fig. 2a-g a clear evolution from the aggregated to the molecularly dissolved states was detected when raising the temperature. The appearance of isosbestic points in the UV spectra points to an equilibrium between monomeric and aggregated species in both cases (see Fig. S4). Very surprisingly, at equal concentrations, **BTT-F** supramolecular polymers revealed higher stability than **BTT-5F** stacks, the monomer with higher hydrophobic component (see Figures S5 and S6).

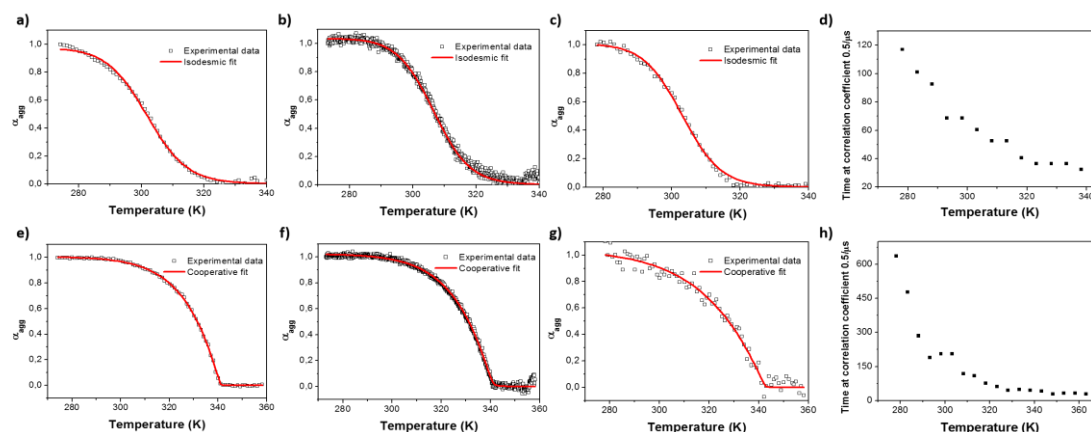


Fig. 2. Fraction of aggregated molecules in water of **BTT-5F** ($c = 5.0 \times 10^{-5}$ M) (top) and **BTT-F** ($c = 1.86 \times 10^{-6}$ M) (bottom) determined by temperature dependent UV ($\lambda = 300$ nm) (a,e), fluorescence ($\lambda_{\text{ex}} = 287$ nm, $\lambda = 400$ nm) (b,f) and CD ($\lambda = 287$ nm) (c,g) spectroscopy cooling from 353 K to 283 K (2 K min^{-1}) (open square) fitted with isodesmic model (up) or cooperative model (bottom) (red line). Temperature dependent DLS of **BTT-5F** ($c = 5.0 \times 10^{-5}$ M) (d) and **BTT-F** ($c = 1.86 \times 10^{-6}$ M) (h).

The higher stability of the monomer endowed with weaker hydrophobic interactions is counterintuitive and deserve further investigation. To this aim, we performed cooling experiments and fit the resulting curves with different models to identify the polymerization mechanism. **BTT-5F** curves obtained by UV, fluorescence and CD lead a clear sigmoidal shape, which can be accurately fitted to a reversible isodesmic polymerization process¹¹ (Figures 2a-c, and S7-S9).

Application of this model to the temperature-dependent curves affords binding constants (K_a) ranging from $3.2 \times 10^4 \text{ M}^{-1}$ to $4.6 \times 10^4 \text{ M}^{-1}$. (See parameters in Table 1).

Table 1. Thermodynamic parameters obtained from the temperature-dependent UV/Vis, Fluorescence and CD experiments of **BTT-5F** in water at different concentrations using an isodesmic model.

BTT-5F	K_a^* [10^4 M^{-1}]	ΔH [kJ mol^{-1}]	ΔS [$\text{Jmol}^{-1}\text{K}^{-1}$]	ΔG [kJ mol^{-1}]
UV ^[a]	5.1	-148	-410	-26.8
F ^[b]	4.7	-150	-414	-26.6
CD ^[c]	5.1	-150	-413	-26.2

[a] $\lambda = 300 \text{ nm}$; [b] ($\lambda_{\text{ex}} = 287 \text{ nm}$, $\lambda = 400 \text{ nm}$); [c] ($\lambda = 287 \text{ nm}$). K_a was calculated at 298 K. The cooling and heating rate was 2 K min^{-1} .

In sharp contrast, the plot of the fraction of aggregated **BTT-F** molecules (α_{agg}) against temperature showed non-sigmoidal curves, suggesting a nucleation-elongation polymerization process (see Figures 2e-g, and S10-S12).⁴ The different melting curves obtained by UV, fluorescence and CD at different concentrations were successfully fitted by the cooperative model developed by Eikelder, Markvoort, Meijer and co-workers¹² (see Table 2).

Table 2. Thermodynamic parameters obtained from temperature-dependent UV/Vis, Fluorescence and CD experiments of **BTT-F** in water at different concentrations on the basis of the ten Eikelder–Markvoort–Meijer model.

BTT-F	ΔH_{ELO} [kJ mol^{-1}]	ΔS [$\text{Jmol}^{-1}\text{K}^{-1}$]	ΔH_{NP} [kJ mol^{-1}]	K_e^* [10^6 M^{-1}]	K_n^* [M^{-1}]	σ^* [10^{-6}]
UV ^[a]	-67	-92	-29	12	84	7.1
F ^[b]	-65	-83	-29	8	61	7.7
CD ^[c]	-58	-60	-28	13	128	9.6

[a] $\lambda = 300 \text{ nm}$; [b] ($\lambda_{\text{ex}} = 287 \text{ nm}$, $\lambda = 400 \text{ nm}$); [c] ($\lambda = 287 \text{ nm}$). * K_n , K_e and σ were calculated at 298 K. The cooling and heating rate was 2 K min^{-1} .

Thermodynamic parameters revealed a 10^6 -fold smaller nucleation constant (K_n) with respect to the elongation step (K_e), indicating a strikingly high degree of cooperativity (σ). Temperature-dependent DLS confirmed that that the loss in CD and UV signal derives from fibers disruption rather than

intramolecular loss of order (see Figures 2d-h). Such a dramatic change of polymerization mechanism between two polymers with very similar structural and spectroscopical properties is crucial for the future design of monomers.

To investigate more in detail the molecular basis of such intriguing difference between these two systems we turned to molecular modeling. We built coarse-grained (CG) models for **BTT-F** and **BTT-5F** monomers according to the same CG scheme recently adopted for similar water-soluble supramolecular polymers (Fig. 3a).¹³

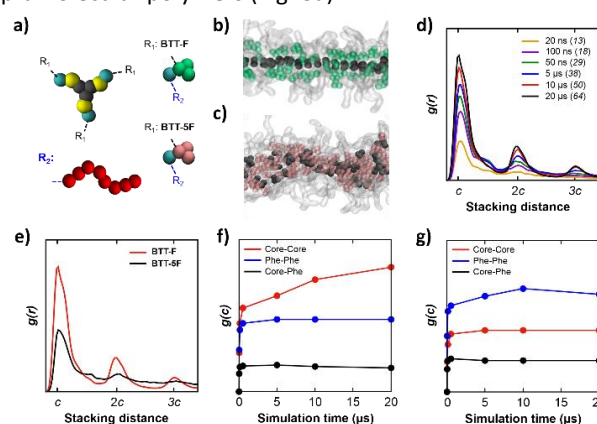


Fig. 3. CG-MD simulations of **BTT-F** and **BTT-5F** self-assembly in water. (a) CG models: core (grey), thiophene (yellow) and amide (cyan) groups, Phe (green), Phe-5F (pink), and PEG (red). (b, c) Detail of cores and Phe in ordered **BTT-F** (c) and disordered **BTT-5F** (d) oligomers (at $20 \mu\text{s}$). (d) Evolution of the $g(r)$ of the **BTT-F** cores in time. (e) Core-core $g(r)$ in **BTT-F** vs. **BTT-5F** ($20 \mu\text{s}$). (f, g) Evolution core-core, Phe-Phe and core-Phe interaction strength ($g(c)$ peak) for **BTT-F** (f) and **BTT-5F** (g).

In particular, the CG models were built and parametrized in order to correctly treat the key factors that control such supramolecular polymers – i.e., behavior of the monomers in solution and the strength of monomer-monomer interactions (see Figures S13 and S14). Similar CG models already proved to correctly treat the cooperativity of the key interactions in supramolecular polymerization, including H-bonding in this case treated implicitly as interaction between the amide CG beads (cyan).^{6,13} CG **BTT-F** and **BTT-5F** models differ only in the beads of the side chains of the aminoacids (Fig. 3a). These are minimally more hydrophobic in **BTT-5F** (pink) than in **BTT-F** (green), consistent with the higher hydrophobicity of fluorinated Phe (see SI). Molecular dynamics (CG-MD) simulations of 160 initially dispersed **BTT-F** or **BTT-5F** monomers into a periodic box filled of explicit water beads allowed to monitor monomer self-assembly in water. After $20 \mu\text{s}$ of CG-MD, long ordered oligomers are spontaneously formed in the **BTT-F** system (see Fig. S15). These fibers are characterized by regular stacking of cores (Fig. 3b). Also, **BTT-**

5F monomers generate elongated aggregates in water, but these are more disordered. Fluorinated-Phe side groups appear tightly compacted in these fibers, impairing the ordered stacking of the **BTT-5F** cores (Fig. 3c). The radial distribution function ($g(r)$) of the cores is an indicator of order into these fibers (the higher the $g(r)$ peaks the more ordered/persistent the stacking).^{6,8d,13} For **BTT-F** system, the $g(r)$ peaks increase with the size of the oligomers during the CG-MD run (Fig. 3d). Such a marked order amplification is even higher than that recently observed in the (cooperative) self-assembly of water-soluble 1,3,5-benzenetricarboxamide (BTA) monomers,^{6,13} proving the strong cooperativity of the **BTT-F** polymerization. Conversely, **BTT-5F** oligomers showed $g(r)$ peaks considerably reduced (Fig. 3e), demonstrating the formation of oligomers with a more disordered internal structure compared to **BTT-F**. We monitored in different ways (see Figures S13 and S14) the relative strength and the evolution during CG-MD of the interactions between the cores, between Phe side chains, and the mixed ones (core-Phe) in both systems. The plots of Figures 3f,g show that the leading interaction in the **BTT-5F** polymerization is between the pentafluoro-L-phenylalanine side chains (Fig. 3g), and not that between the cores as in **BTT-F** (Fig. 3f). This explains why **BTT-5F** tends to form more disordered oligomers as opposed to **BTT-F** (Figures 3b,c). All interactions well equilibrate in the regime of these CG-MD simulations, with the exception of the core-core interaction in system **BTT-F** that continues to increase (Fig. 3f: red). The cooperativity of core-core interactions is thus at the origin for the striking cooperative mechanism of polymerization of **BTT-F**, while all interaction in the **BTT-5F** system are well compatible with an isodesmic polymerization mechanism. Interestingly, molecular modelling results correlate well with Nile Red (NR) spectroscopy assays. NR mixed with **BTT-5F** showed a clear increase of fluorescence due to NR intercalation between discs (see Figures S16 and S17). On the contrary, NR fluorescence was only slightly increased when incubating NR with **BTT-F**. This fact is probably indicating that **BTT-F** monomers pack very compactly and NR cannot get intercalated.

In summary, we have rationally designed two different water-soluble BTT derivatives and studied their self-assembly into one-dimensional fibers. The polymerization of both monomers is driven by a delicate combination of hydrogen bonding and hydrophobic effects. While **BTT-5F** isodesmic self-assembly is dominated by hydrophobic forces leading to internally disordered single fibers, **BTT-F** self-assembly evolves via a highly cooperative polymerization mechanism due to the greater contribution of directional H-bonding and core-stacking forces, affording highly ordered one-dimensional fibers. This work provides a clear structure-property relationship, providing a useful tool to control the polymerization mechanism of the monomers, and consequently, the final properties of the fibers.

Financial support from Comunidad de Madrid, Spain (S2013/MIT- 2841, FOTOCARBON) and Spanish MICINN (CTQ2014-52869-P) (T.T.) is acknowledged. This work was also financially supported by the Spanish MICINN through the

project SAF2016-75241-R (L.A., S.P.) and by the Generalitat de Catalunya through the CERCA program. G.M.P. acknowledges the Swiss National Science Foundation (SNSF grant: 200021_162827).

Conflicts of interest

There are no conflicts to declare.

Notes and references

- (a) E. Krieg, B. Rybtchinski, *Chem. - Eur. J.*, 2011, **17**, 9016; (b) S. I. Stupp, *Nano Lett.* 2010, **10**, 4783; (c) D. Chandler, M. J. Webber, E. A. Appel, E. W. Meijer, R. Langer, *Nat. Mater.*, 2015, **15**, 13.
- (a) C. M. A. Leenders, L. Albertazzi, T. Mes, M. M. E. Koenigs, A. R. A. Palmans, E. W. Meijer, *Chem. Commun.*, 2013, **49**, 1963; (b) M. B. Baker, L. Albertazzi, I. K. Voets, C. M. A. Leenders, A. R. A. Palmans, G. M. Pavan, E. W. Meijer, *Nat. Commun.*, 2015, **6**, 6234; (c) Bochicchio, D.; Salvalaglio, M.; Pavan, G. M. *Nat. Commun.*, 2017, **8**, 147.
- E. Krieg, M. M. C. Bastings, P. Besenius, B. Rybtchinski, *Chem. Rev.*, 2016, **116**, 2414.
- T. F. A. de Greef, M. M. J. Smulders, M. Wolffs, A. P. H. J. Schenning, R. P. Sijbesma, E. W. Meijer, *Chem. Rev.*, 2009, **109**, 5687.
- C. Kulkarni, K. K. Bejagam, S. P. Senanayak, K. S. Narayan, S. Balasubramanian, S. J. George, *J. Am. Chem. Soc.*, 2015, **137**, 3924.
- D. Bochicchio, G. M. Pavan, *ACS Nano*, 2017, **11**, 1000.
- (a) C. Rest, R. Kandaneli, G. Fernández, *Chem. Soc. Rev.*, 2015, **44**, 2543; (b) C. Kulkarni, E. W. Meijer, A. R. A. Palmans, *Acc. Chem. Res.*, 2017, **50**, 1928.
- (a) N. K. Allampally, A. Florian, M. J. Mayoral, C. Rest, V. Stepanenko, G. Fernández, *Chem. A Eur. J.*, 2014, **20**, 10669; (b) P. Besenius, G. Portale, P. H. H. Bomans, M. Janssen, A. R. A. Palmans, E. W. Meijer, *Proc. Natl. Acad. Sci.*, 2010, **107**, 17888; (c) C. Rest, M. J. Mayoral, K. Fucke, J. Schellheimer, V. Stepanenko, G. Fernández, *Angew. Chem., Int. Ed.*, 2014, **53**, 700; (d) Garzoni, M.; Baker, M. B.; Leenders, C. M. A.; Voets, I. K.; Albertazzi, L.; Palmans, A. R. A.; Meijer, E. W.; Pavan, G. M. *J. Am. Chem. Soc.*, 2016, **11**, 13985.
- (a) A. Demenev, S. H. Eichhorn, *Chem. Mater.*, 2010, **22**, 1420–1428; (b) X. Guo, S. Wang, V. Enkelmann, M. Baumgarten K. Müllen, *Org. Lett.*, 2011, **13**, 6062.
- C. F. C. Spano, *Acc. Chem. Res.*, 2010, **43**, 429.
- M. M. Smulders, M. M. L. Nieuwenhuizen, T. F. A. De Greef, P. van der Schoot, A. P. H. J. Schenning, E. W. Meijer, *Chem. Eur. J.*, 2010, **16**, 362.
- A. J. Markvoort, H. M. M. ten Eikelder, P. A. J. Hilbers, T. F. A. de Greef; E. W. Meijer, *Nat. Commun.*, 2011, **2**, 509.
- Bochicchio, D.; Pavan, G. M. *J. Phys. Chem. Lett.*, 2017, **8**, 3813.